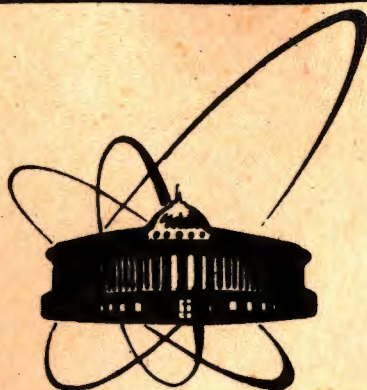


92-212



ОБЪЕДИНЕННЫЙ
ИНСТИТУТ
ЯДЕРНЫХ
ИССЛЕДОВАНИЙ
ДУБНА

E4-92-212

N.V.Antonenko, E.A.Cherepanov, A.K.Nasirov*,
V.P.Permjakov, V.V.Volkov

ANALYSIS OF COMPOUND
NUCLEUS FORMATION
IN REACTIONS $^{100}\text{Mo} + ^{100}\text{Mo}$ AND $^{110}\text{Pd} + ^{110}\text{Pd}$.
FUSION BARRIER

Submitted to "Z.Phys.A — Hadrons and Nuclei"

*Institute of Nuclear Physics, Uzbekistan

1992

1. Introduction

The mechanism of the compound nucleus formation (CNF) in heavy ion-induced reactions is of considerable interest. But its experimental investigation is very difficult since during the complete fusion the system does not give signals which allow one to judge about this process unambiguously. In experiments, the decay products of an excited compound nucleus are registered, however they contain no information about the mechanism of the CNF. A consistent theoretical analysis of the complete fusion process of two multinucleon interacting system is a very complicated problem. Therefore a number of models have been developed for the description of the experimental data. These models are based on simplifying assumptions about the fusion process.

The critical distance model [1], optical model [2] and the surface friction model [3,4] widely used for the calculation of fusion cross sections do not consider the mechanism of CNF itself. It is postulated that after the capture of a projectile by a target nucleus the complete fusion occurs inevitably. One can say sometimes that the process of compound nucleus formation looks like the nuclear collapse. The macroscopic dynamic model [5-7] allows us to trace the evolution of the fusion system in time. However, such important properties of nuclei as their nucleon composition and shell structure are not taken into account. In replacing the real atomic nuclei by homogeneous and structureless drops of a hypothetical nuclear liquid, the real process of the compound nuclei formation is inevitably distorted.

In [8] a new approach to the analysis of the complete fusion process has been suggested. This approach is based on the information about the interaction of two complex nuclei being in close contact, which has been obtained in the study of deep inelastic transfer reactions. In the framework of this approach the complete fusion of the nuclei is interpreted in the following way. At the capture stage after the full dissipation of the collision kinetic energy a dinuclear system (DNS) is formed. The DNS evolves to a compound nucleus by the nucleon transfer from a light nucleus to a heavy one. An important peculiarity of the DNS evolution is the retaining of the individuality of nuclei through their way to the compound nucleus formation. During the DNS evolution all nucleons of the donor-nucleus occur to be transferred shell by shell to the acceptor-nucleus. For brevity we will call this approach the "DNS-approach".

The data on the complete fusion of massive nuclei are very useful for revealing the mechanism of the compound nucleus formation. Namely, in the case of massive nuclei,

the calculations of the cross section of compound nucleus formation in the framework of various models give largely divergent results. The comparison of the calculated and experimental data allows us to estimate the validity of various complete fusion models.

In this work the experimental data [9] on evaporation residues cross sections for reactions $^{100}\text{Mo}+^{100}\text{Mo}$ and $^{110}\text{Pd}+^{110}\text{Pd}$ are compared with results calculated in the framework of the traditional models: the optical model [2], the surface friction model [4], the macroscopic dynamic model [7] (Sect.2). The calculations include the determination of the cross section of compound nucleus formation and the analysis of the competition between various de-excitation channels. The calculated results are in dramatic discrepancy with the experimental data. For the reaction $^{110}\text{Pd}+^{110}\text{Pd}$ the calculated data is several orders of magnitude more than the experimental one. On the contrary the calculations in the framework of the DNS-approach (Sect.3) give the best agreement with the experimental results. This fact can be considered as an indication of the validity of the interpretation of the compound nucleus formation mechanism suggested in the DNS-approach.

2. Calculation of evaporation residue cross sections in reactions $^{100}\text{Mo}+^{100}\text{Mo}$ and $^{110}\text{Pd}+^{110}\text{Pd}$ in the framework of traditional models of complete fusion

2.1 Calculation of compound nucleus formation cross section in the framework of the optical model

The CNF cross section was estimated by one of the variants of the optical model that was used for the description of experimental data on the synthesis of transuranium elements [2,10]. The model parameters have been systematized in a wide region of $Z_1 \cdot Z_2$ by comparing results of calculation with the experimental data.

The CNF cross section σ_{CN} is a part of the total reaction cross section σ_R

$$\sigma_R = \pi \lambda_0^2 \sum_{l=0}^{\infty} (2l+1) \cdot T(l, E_{cm}). \quad (1)$$

Here λ_0 is the de Broglie wave length of the relative motion of interacting nuclei, E_{cm} is the bombarding energy in the center of mass system, T is the penetration coefficient of the l -th partial wave through the potential barrier V_l . The potential describing the

nucleus-nucleus interaction includes nuclear, Coulomb, and centrifugal potentials

$$V(R) = V_N + V_C + V_r, \quad (2)$$

$$V_N = V_0 \left\{ 1 + \exp \left[\frac{R - r_{0v}(A_1^{1/3} + A_2^{1/3})}{d} \right] \right\}^{-1}, \quad (3)$$

$$V_C = \begin{cases} Z_1 Z_2 e^2 / R, & \text{if } R > R_C, \\ Z_1 Z_2 e^2 / 2R_C (3 - R^2/R_C^2), & \text{if } R \leq R_C, \end{cases} \quad (4)$$

$$V_r = \hbar^2 l(l+1) / 2\mu R^2, \quad (5)$$

where R is the distance between nuclear centres; $R_C = 1.3(A_1^{1/3} + A_2^{1/3})$ fm, μ is the reduced mass of the system. The quantities corresponding to the projectile and target nuclei are marked by indices 1 and 2, respectively. The potential parameters V_0 , r_{0v} and d are taken from [11]. The value of the CNF cross section σ_{CN} could be found by calculating σ_R and using the empirical systematics of the ratio σ_{CN}/σ_R presented in [2]. In the region $Z_1 \cdot Z_2 < 1500$ the experimental values of σ_{CN}/σ_R can be approximated by the two expressions:

$$\sigma_{CN}/\sigma_R = (1 + 5 \cdot 10^{-4} Z_1 Z_2)^{-1}, \quad (6)$$

$$\sigma_{CN}/\sigma_R = [(0.945 \pm 0.055) - 2.7 \cdot 10^{-4} Z_1 Z_2]. \quad (7)$$

which give the same accuracy within the experimental error. In the calculations of σ_{CN} for a heavier system with $Z_1 \cdot Z_2 > 1500$, the energy displacement between the fusion barrier B_{fus} and the interaction barrier B_{int} should be taken into account. In the present paper this is done according to [11]. The results for CNF cross sections in the reactions $^{100}\text{Mo}+^{100}\text{Mo}$ and $^{110}\text{Pd}+^{110}\text{Pd}$ calculated in the framework of the optical model are presented in Figs.1 and 2.

2.2 Calculation of the CNF cross section in the framework of the surface friction model

The complete fusion is assumed to take place in the surface friction models if the nuclei after full dissipation of the collision kinetic energy are captured in the attractive potential. By introducing the nuclear friction and solving the system of classical equations of motion we can obtain the critical angular momentum l_f . All the trajectories with $l < l_f$ lead to the compound nucleus formation. In the sharp cut off approximation the cross section is determined by the expression:

$$\sigma_{CN} = \pi \lambda_0^2 \sum_{l=0}^{l_f} (2l+1) = \pi \lambda_0^2 (l_f + 1)^2. \quad (8)$$

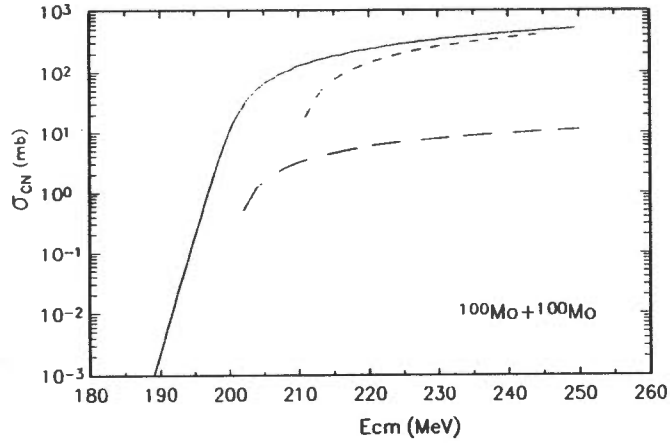


Fig.1. Calculated cross sections of compound nucleus formation for the reaction $^{100}\text{Mo}+^{100}\text{Mo}$ in the framework of optical model (solid line), surface friction model (short dashed line) and macroscopic dynamic model (long dashed line), as a function of center of mass energies.

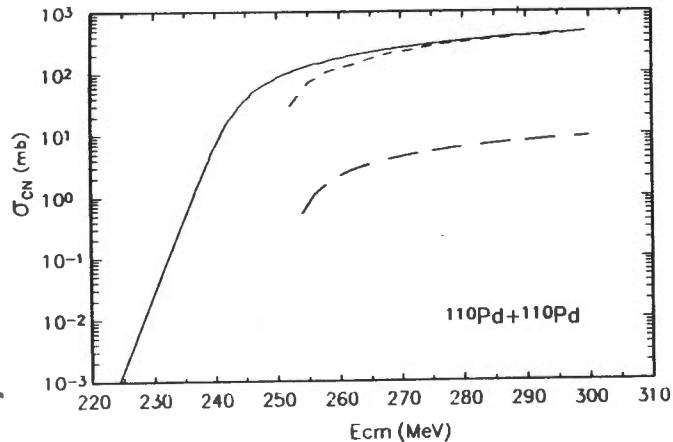


Fig.2. Same as Fig. 1, but for the reaction $^{110}\text{Pd}+^{110}\text{Pd}$

The calculations are based on one of the recent variants of the surface friction model which takes into account the dynamic deformation of both the colliding nuclei [4]. It should be noted that in the framework of this model the capture cross section can be satisfactorily described for such a massive ion as ^{86}Kr .

The system of classical equations of motion was obtained in [4] using the Lagrangian \mathcal{L} , taking into account the coupling of the relative motion with quadrupole vibrations and using the Rayleigh dissipative function \mathcal{R} :

$$\frac{d}{dt} \frac{\partial \mathcal{L}}{\partial \dot{q}_i} - \frac{\partial \mathcal{L}}{\partial q_i} + \frac{\partial \mathcal{R}}{\partial \dot{q}_i} = 0. \quad (9)$$

$$\mathcal{L} = \frac{p_R^2}{2\mu} + \frac{l^2}{2\mu R^2} \sum_i \left(\frac{\pi_i^2}{2D_i} - \frac{1}{2} C_i \alpha_i^2 \right) - V(R, \alpha_i). \quad (10)$$

Here q_i are the generalized coordinates, p_R is the radial momentum, α_i are the deformation parameters, π_i are the conjugate momenta, D_i and C_i are the mass coefficients and the hardness parameters for quadrupole vibrations, $V(R, \alpha_i)$ is a conservative potential being a sum of the nuclear and the Coulomb potentials [4].

For the dissipative function the following expression is used:

$$\mathcal{R} = \frac{1}{2} K_R \dot{R}^2 + \frac{1}{2} K_\Phi R^2 \dot{\Phi}^2 + \sum_i K_{R\alpha_i} \dot{R} \dot{\alpha}_i + \frac{1}{2} \sum_{i,j} K_{\alpha_i \alpha_j} \dot{\alpha}_i \dot{\alpha}_j, \quad (11)$$

where

$$K_R = K_R^0 \left(\frac{\partial V_N(R, \alpha_i)}{\partial R} \right)^2, \quad K_\Phi = K_\Phi^0 \left(\frac{\partial V_N(R, \alpha_i)}{\partial R} \right)^2, \\ K_{R\alpha_i} = -R_i Y_{20}, \quad K_{\alpha_i \alpha_j} = R_i R_j Y_{20}^2 K_R + K_{\alpha_i}^0 (C_i D_i)^{1/2} \delta_{ij},$$

R_i ($i=1,2$) are the radii of spherical nuclei. The values of the coefficients K_Φ^0 , $K_{\alpha_i}^0$, K_R^0 are fixed in [4] for all the analysed reactions

$$K_\Phi^0 = 0.01 \cdot 10^{-23} (\text{s/MeV}), \quad K_R^0 = 3.5 \cdot 10^{-23} (\text{s/MeV}), \quad K_{\alpha_i}^0 = 20.$$

The calculated cross sections of the CNF within the surface friction model for the reactions $^{100}\text{Mo}+^{100}\text{Mo}$ and $^{110}\text{Pd}+^{110}\text{Pd}$ are presented in Figs.1 and 2. At high collision energies they are close to the results of the optical model, but at lower energies we have obtained lower values for σ_{CN} . As is known the surface friction model is used in the calculations of σ_{CN} for the energies above the Coulomb barrier.

2.3 Calculation of the CNF cross section in the framework of the macroscopic dynamic model

A recent variant of the macroscopic dynamic model [7] has been used to calculate the CNF cross section in the reactions $^{100}\text{Mo}+^{100}\text{Mo}$ and $^{110}\text{Pd}+^{110}\text{Pd}$. In this model σ_{CN} is determined by the following expression:

$$\sigma_{CN}(E_{cm}) = \frac{\pi r_c^2}{E_{cm}} \left[\sqrt{\left(\frac{c_1 c_2 + 0.5}{c_2^2} \right)^2 - \left(\frac{c_1^2 + E_B - E_{cm}}{c_2^2} \right)} - \left(\frac{c_1 c_2 + 0.5}{c_2^2} \right) \right], \quad (12)$$

where

$$c_1 = k^{1/2} [(Z^2/A)_{ef} - (Z^2/A)_{ef}^{thr}], \quad c_2 = \frac{k^{1/2}}{e^2/r_0} \frac{8f^2}{(A_1 A_2)^{1/3}}$$

$$k = 2025 \cdot (A_1 A_2)^{1/3} (A_1^{1/3} + A_2^{1/3})^2 32 \left(\frac{3}{\pi} \right)^{2/3} mc^2 a^2 / (A_1 + A_2)$$

$$r_c = D_1 + D_2 + 1.44 \text{ fm}, \quad D_i = R_i - 1/R_i,$$

$$R_i = 1.28 A_i^{1/3} - 0.76 + 0.8 A_i^{-1/3}, \quad mc^2 = 931 \text{ MeV}, \quad r_0 = 1.224 \text{ fm}.$$

In [7] the following values for parameters are recommended for better description of the experimental data:

$$f = 3/4, \quad a = 12, \quad (Z^2/A)_{ef}^{thr} = 33.$$

The calculated σ_{CN} for both reactions are presented in Figs.1,2. In comparison with the optical and the surface friction models the macroscopic dynamic model gives lower values for σ_{CN} , and the excitation function seems to be shifted to higher energies of ions. Since in the macroscopic dynamic model the CNF cross section σ_{CN} does not coincide with the capture cross section σ_C , we obtain a smaller probability of the compound nucleus formation. After the capture stage a massive dinuclear system goes into the quasifission channel with a great probability. The shift of the cross sections to higher energies may be connected with the overestimation of the extra-extra push energy [4].

2.4 Calculation of evaporation residue cross sections

In the reactions $^{100}\text{Mo}+^{100}\text{Mo}$ and $^{110}\text{Pd}+^{110}\text{Pd}$ the compound nuclei ^{200}Po and ^{220}U are formed with the excitation energy of dozens MeV and with a large set of angular momenta. The competition between fission and emission of the light particle determines the part of compound nuclei surviving as evaporation residues.

To describe the decay of excited nuclei ^{200}Po and ^{220}U , a statistical model based on the Monte-Carlo method has been used. The angular momenta of compound nuclei formed in the complete fusion reaction have a respective distribution of value of I . The vector \mathbf{I} is oriented transversal to the ion beam. By means of two random numbers the drawing of the momentum value and its orientation in space is performed. Then for different decay channels of the compound nucleus the maximum of residual energy is defined in the following way

$$E_\nu^{max} = E^* - E_r - E_\nu - V_\nu; \quad E_f^{max} = E^* - E_r - B_f.$$

Here E^* is the excitation energy of the compound nucleus, E_r is its rotational energy, V_ν is the exit Coulomb barrier for a particle of the kind ν , E_ν is the kinetic energy of the particle, B_f is the fission barrier. For all $E_\nu^{max} > 0$ the kind of the emitted particle or γ -ray is drawn. For partial widths of the particle ν emission, for the fission and of the γ -quanta emission the following expressions have been used [12]:

$$\Gamma_\nu(E_H^*, I_H) \approx -\frac{2(2s_\nu + 1)}{\pi^2 \hbar^3 \rho_H(U)} \int_{V_\nu}^{U-B_\nu} \sigma_{inv}(E_\nu) \rho_K(U - B_\nu - E_\nu) E_\nu dE_\nu, \quad (13)$$

$$\Gamma_f(E_H^*, I_H) \approx (2\pi \rho_H(U))^{-1} \int_0^{U-B_\nu} \rho_s(U_s - B_f - \epsilon) d\epsilon, \quad (14)$$

$$\Gamma_\gamma(E_H^*, I_H) \approx \frac{3}{(\pi \hbar c)^2 \rho_H(U)} \int_0^U \sigma_{\gamma A}(E_\gamma) \rho_K(U - E_\gamma) E_\gamma^2 dE_\gamma, \quad (15)$$

where U is the thermal energy of the nucleus. The inverse cross section σ_{inv} is calculated within the optical model [13]:

$$\sigma_{inv} = \begin{cases} \sigma_g c_1 (1 + c_2/E_\nu), & \nu = n, \\ \sigma_g c_3 (1 + c_4 V_\nu/E_\nu), & \nu = p, d, t, {}^3\text{He}, \alpha. \end{cases} \quad (16)$$

Here σ_g is the geometrical cross section, r , c_1 , c_2 , c_3 , c_4 are the parameters taken from [13]. In expression (14) the thermal energy U_s and rotational energy E_r^* are connected at the saddle point by the relation $U_s = E^* - E_r^*$. This form of the width Γ_f takes into account the change of the fission barrier of rotating nucleus so far as $B_f(I) = B_f(0) - (E_r - E_r^*)$ (see details in [14]). In expression (14) for the partial width of the electric dipole radiation $\sigma_{\gamma A}$ is the photoabsorbtion cross section.

To describe the level density as a function of the excitation energy, the well known

expression from [15]

$$\rho(E^*) = \frac{\sqrt{\pi}}{12} \frac{1}{a^{1/4}(E^*)^{5/4}} \exp[S(E^*)], \quad (17)$$

has been used. In (17) the dependence of the nucleus entropy S on the excitation energy E^* is determined by the relation

$$S = 2at \quad (18)$$

by using the coupling of the nucleus temperature with its excitation energy:

$$E^* = at^2 \quad (19)$$

The parameter of the level density $a = \pi g_0^2/6$ is expressed through the density of single particle states near the Fermi energy $g_0 = g(E_f) = \text{const}$. The decrease of shell effects influence on the levels density with increasing excitation energy is taken into account by the phenomenological expression [15]:

$$a(E^*) = \bar{a}[1 + f(E^*)\delta W/E^*], \quad (20)$$

Here $f(x) = 1 - \exp(-\gamma x)$, and δW is the shell correction in the nucleus mass formula, $\bar{a} = A(\alpha + \beta A)$ is the Fermi-gas value of the level density parameter. The empirical values of the parameters $\alpha = 0.134 \text{ MeV}^{-1}$, $\beta = -1.21 \cdot 10^{-4} \text{ MeV}^{-1}$, $\gamma = 6.1 \cdot 10^{-2} \text{ MeV}^{-1}$ have been obtained from the analysis of the data on the levels density with taking account the contribution of the collective states to total levels density:

$$\rho_{\text{tot}}(E^*) = E_{\text{rot}} K_{\text{vib}} \rho(E^*) \quad (21)$$

(see details in [15]).

After the determination of the de-excitation mode (if fission does not occur) the characteristics of the emitted particles or γ -ray, namely their kinetic energy, orbital momentum and emission angle were drawn. For the given kind of the particle the simultaneous selection of E_ν , l and $\cos(\Theta)$ has been performed by using the three random numbers. Then by using the fourth random number they are rejected according to the three-dimensional probability density.

$$W(E_\nu, l, \cos(\Theta)) \simeq l \exp \left[2\sqrt{a(E_k^* - E_\nu - (I^2 + l^2)/2J + Il \cos(\Theta)/J)} \right], \quad (22)$$

Here J is the moment of inertia of the compound nucleus. The azimuthal angle of the evaporated particle is drawn in the coordinate system with the axis z parallel to I . The fission process is taken into account by the weight function

$$FU = \prod_{\nu=1}^x [1 - \Gamma_f/\Gamma_{\text{tot}}], \quad (23)$$

This is convenient, in particular, for strongly fissionable nuclei. All the quantities are transformed to the centre of mass system of interacting nuclei and the characteristics of the residual nucleus

$$\begin{aligned} I_f &= I - l; & E_{\text{res}}^* &= E^* - B_\nu - E_\nu - (I_f^2 - l^2)/2 \cdot J; \\ A_{\text{res}} &= A_{CN} - A_\nu; & Z_{\text{res}} &= Z_{CN} - Z_\nu. \end{aligned} \quad (24)$$

are calculated. Then the maximum residual energies of all emission processes and fission channels are calculated for this nucleus. Among the allowed values of E_ν^{max} and $E_f^{\text{max}} > 0$ the next drawing of the de-excitation type is performed. This is done while the condition $E_{\text{res}} > 0$ is satisfied. The gathering of the required statistics for the calculation of different reaction characteristics has provided the about 5% calculation accuracy.

The computation of the compound nucleus de-excitation on the basis of the Monte-Carlo method is performed for all the considered variants of the CNF cross section calculation (see sections 2.1, 2.2, 2.3). The calculated evaporation residue cross sections in the reactions $^{100}\text{Mo} + ^{100}\text{Mo}$ and $^{110}\text{Pd} + ^{110}\text{Pd}$ are compared in Figs.3.4 with the experimental data [9]. Strong discrepancy is observed between the calculated and the experimental results. The discrepancy is particularly large for the reaction $^{110}\text{Pd} + ^{110}\text{Pd}$ when the CNF cross section is calculated within the optical model and the surface friction model. The macroscopic dynamic model gives lower values of σ_{CN} , but the discrepancy between the calculated results and the experimental data is several orders of magnitude. The observed discrepancy cannot be explained in the framework of the traditional concepts of the fusion of complex nuclei. Therefore we have tried to investigate the reason of strong decrease of the evaporation residue cross sections in these reactions using the DNS-approach.

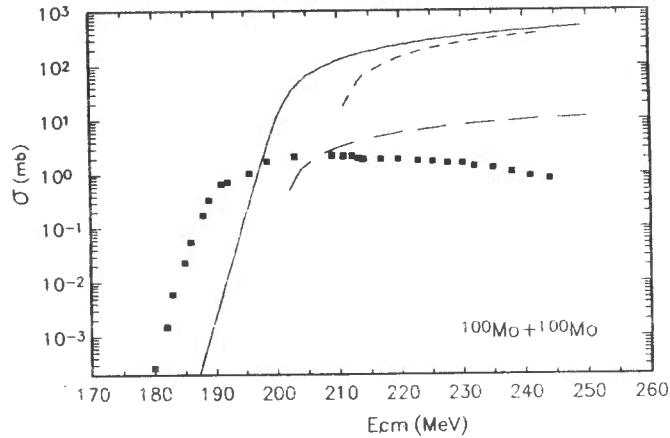


Fig.3. Calculated evaporation residue cross sections for the reaction $^{100}\text{Mo}+^{100}\text{Mo}$ in the framework of optical model (solid line), surface friction model (short dashed line) and macroscopic dynamic model (long dashed line), as a function of center of mass energies. The experimental data are presented by solid squares

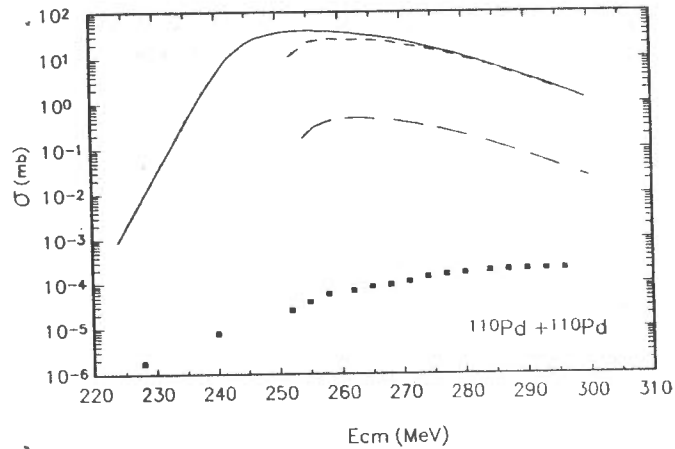


Fig.4. Same as Fig. 3, but for the reaction $^{110}\text{Pd}+^{110}\text{Pd}$

3. Calculation of the evaporation residue cross sections in the reactions $^{100}\text{Mo}+^{100}\text{Mo}$ and $^{110}\text{Pd}+^{110}\text{Pd}$ in the framework of the DNS - approach.

3.1 Peculiarity of the complete fusion of the massive nuclei. Fusion barrier

According to the DNS-approach the first stage of the complete fusion of nuclei ends by the formation of the DNS. The DNS evolution is defined by the potential energy $V(Z, l)$ of the system as a function of its charge asymmetry and the collision angular momentum. In Figs.5,6 the potential energy of the DNS for the reactions $^{100}\text{Mo}+^{100}\text{Mo}$ and $^{110}\text{Pd}+^{110}\text{Pd}$ is presented. The liquid-drop mass of nuclei [16] and nucleus-nucleus potential (2) are used in the calculation of $V(Z, l)$. The calculation has been performed under a simple assumption about the DNS form. The DNS is considered as two spherical overlapping nuclei. The distance R between their centres corresponds to the position of the minimum of potential packet of $V(R)$. The retaining individuality of nuclei during the DNS evolution to a compound nucleus [8] allows us to use this assumption in the calculation. The energy scales are normalized to the total energy of the corresponding spherical compound nucleus. The isotopic composition of the nuclei forming the DNS is chosen from the condition of N/Z equilibrium in the system.

The nuclear interaction $V_N(R)$ is taken in two variants: "proximity" and "folding". According to [17] the expression for $V_N(R)$ in the "proximity" variant looks like:

$$V_N(R) = -2\pi(\gamma_1 + \gamma_2)\bar{R}s_0 \begin{cases} \frac{5}{3}(1 + s/s_0)\exp[-1.6s/s_0], & s \geq 0, \\ \frac{5}{3} - s/s_0 - \frac{1}{2}(s/s_0)^2, & s < 0, \end{cases} \quad (25)$$

where

$$\begin{aligned} \gamma_i &= 0.9517(1 - 1.7826(1 - 2Z_i/A_i)^2), \\ R_{ip} &= 1.17A^{1/3}, \\ s &= R - R_{1p} - R_{2p}, \quad s_0 = 1\text{fm} \end{aligned}$$

Here s is the distance between the surfaces of interacting spherical nuclei,

$$\bar{R} = \frac{R_{1p}R_{2p}}{R_{1p} + R_{2p}}.$$

The expression for $V_N(R)$ in the "folding" form is taken from [19]

$$V_N(R) = \int \omega_1(\mathbf{r}_1)\omega_2(\mathbf{R} - \mathbf{r}_2)\mathcal{F}(\mathbf{r}_1 - \mathbf{r}_2)d\mathbf{r}_1d\mathbf{r}_2. \quad (26)$$

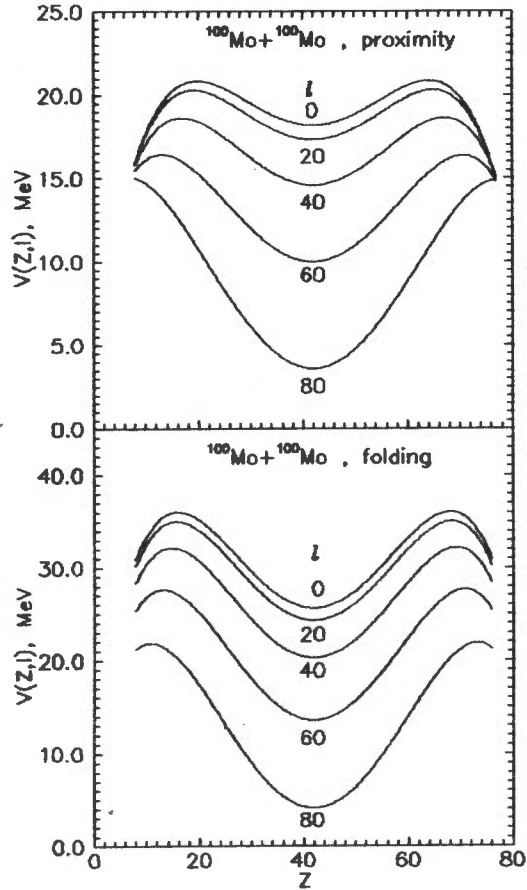


Fig.5. Potential energy of the dinuclear system as a function of its charge asymmetry at different angular momenta in the case of reaction $^{100}\text{Mo}+^{100}\text{Mo}$. The nuclear interaction is taken in proximity (*upper part*) and double folding (*bottom part*) forms

Here $\omega_i(\mathbf{r}_i)$ are the densities of interacting nuclei, $\mathcal{F}(\mathbf{r}_1 - \mathbf{r}_2)$ is the nucleon-nucleon interaction potential. To take into account the repulsive part of the nucleus-nucleus potential, we used the density depending nucleon-nucleon forces [18]. The final expression has the form [19]:

$$V_N(R) = C_0 \left\{ \frac{F_{in} - F_{ex}}{\omega_{00}} \left(\int \omega_1^2(\mathbf{r})\omega_2(\mathbf{r} - \mathbf{R})d\mathbf{r} + \int \omega_1(\mathbf{r})\omega_2^2(\mathbf{r} - \mathbf{R})d\mathbf{r} \right) + F_{ex} \int \omega_1(\mathbf{r})\omega_2(\mathbf{r} - \mathbf{R})d\mathbf{r} \right\}, \quad (27)$$

$$F_{in,ex} = f_{in,ex} + f'_{in,ex}(N_1 - Z_1)/A_1(N_2 - Z_2)/A_2,$$

where N_i are the neutron numbers. The values of the dimensionless parameters f, f'

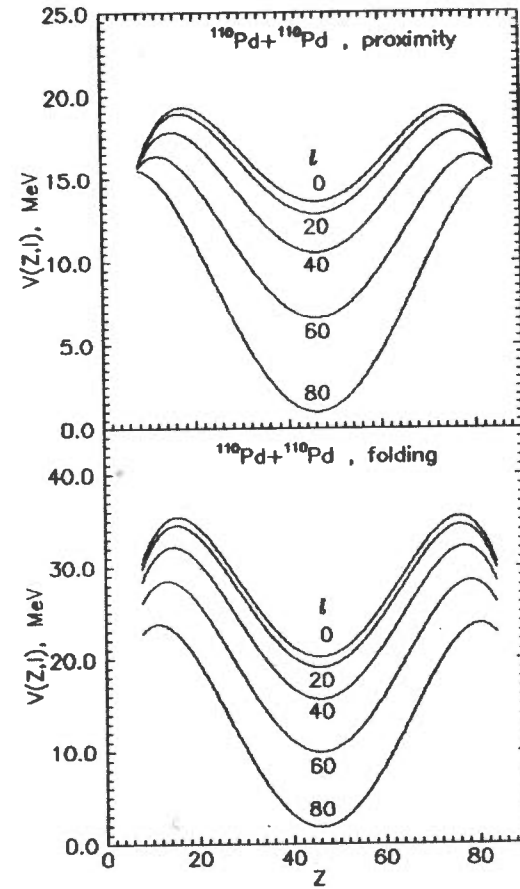


Fig.6. Same as Fig. 5, but for the system $^{110}\text{Pd}+^{110}\text{Pd}$

are known from the fit of a great set of the experimental data within the theory of the finite Fermi-system [18]:

$$C_0 = 300 \text{ MeV fm}^3, f_{in} = 0.09, f_{ex} = -2.59, f'_{in} = 0.42, f'_{ex} = 0.54.$$

For massive nuclei the following expression can be used:

$$\omega_i(\mathbf{r}) = \frac{\omega_{00}}{(1 + \exp((r - R_{i0})/a_0))} \quad (28)$$

with parameters $\omega_{00} = 0.17 \text{ fm}^{-3}$, $R_{i0} = r_0 A_i^{1/3}$. The position and height of the barrier for many reactions are well described by the values of parameters $r_0 = (1.08 \div 1.17) \text{ fm}$ and $a_0 = (0.45 \div 0.55) \text{ fm}$ [19].

A partial overlapping of the volumes of interacting nuclei [20] is taken into account in the Coulomb potential. A complete sticking takes place for the DNS evolving to

the compound nucleus, therefore the centrifugal potential $V_r(R)$ has the form:

$$V_r(R) = \frac{\hbar^2 l(l+1)}{2(j_1 + j_2 + \mu R^2)}, \quad (29)$$

where $j_i = 2mA_i R_i^2/5$ are the rigid bodies moments of inertia of the DNS nuclei.

As it is seen from Figs.5,6, in both the reactions the initial DNS seem to be at the minimum of the potential energy. The DNS is similar to the giant nuclear molecule. As it has been emphasized in [8], the existence of the shell structure gives significant stability to nuclei of DNS. By exchanging the valence nucleons the nuclei of the DNS retain their individuality in a wide range. The excitation energy of the DNS is determined by the collision kinetic energy and nucleus-nucleus potential in the reaction entrance channel. In the massive DNS several types of nuclear processes can occur. Firstly, the evaporation of light fragments and γ -ray since the excitation energy of the system is dozens of MeV. The evaporation of light particles leads to the cooling of the system. Secondly type, strong Coulomb forces, acting between the nuclei, raise the deformation of the system increasing in time. As a result, the system can decay into two nuclear fragments with nearly equal masses. So far as the compound nucleus formation does not precede the decay of the system, this is a quasifission process. Finally, due to the redistribution of nucleons between the DNS nuclei, the configuration of the DNS corresponding to the Businaro-Gallone (BG) point can arise. After this point DNS evolves to the compound nucleus.

It is clear from Figs.5,6 that on its way to the compound nuclei the DNS has to overcome the potential barrier $\delta V(l)$ that is equal to the difference of the potential energy $V(Z, l)$ at the BG point and symmetric configuration. This difference can be called the fusion barrier B_{fus} . Even at a considerable surplus kinetic energy over the entrance barrier the fusion barrier appears on the way to the compound nucleus. This is a specific feature of the complete fusion of massive nuclei which is revealed only within the DNS-approach.

It is necessary to emphasize once more that even at collisions with zero angular momentum in the driving potentials the fusion barrier exists for a massive nuclear system due to the conservation of nucleus individuality in the evolution of the DNS to a compound nucleus.

The physical nature of this fusion barrier drastically differs from the extra-extra push of the macroscopic dynamic model [5-7]. The extra-extra push is an additional kinetic energy over the entrance potential barrier which should be provided to ensure the compact form of fusing nuclei, i.e. a more compact form than the form of the fissile

compound nucleus at the saddle point has to be reached. Unlike the extra-extra push, the source of energy for getting over the fusion barrier B_{fus} is the DNS excitation energy. Namely, the excitation energy allows the system to realize such an endoergic redistribution of the nucleons between the DNS nuclei after which the system turns out to be on top of the fusion barrier. After reaching the fusion barrier the DNS potential energy begins to decrease with increasing charge asymmetry and the driving forces incite the DNS evolution to a compound nucleus.

Thus, in the calculations of evaporation residue cross sections in the reactions $^{100}\text{Mo} + ^{100}\text{Mo}$ and $^{110}\text{Pd} + ^{110}\text{Pd}$ we have to take into account:

- a) the competition between the quasifission and the complete fusion at the CNF;
- b) the competition between the fission and the nucleon, α -particle, γ -ray emission in the de-excitation of a compound nucleus.

3.2 Calculation of the cross section of compound nucleus formation in the reactions $^{100}\text{Mo} + ^{100}\text{Mo}$ and $^{110}\text{Pd} + ^{110}\text{Pd}$ in the framework of the DNS-approach

The capture cross sections σ_c for both the reactions are calculated in the framework of the optical model. Our calculation of the competition between the quasifission and the complete fusion was based on the fact that the initial DNS is at the minimum of the potential energy. Accordingly the paper [21] the decay of the nuclear system through quasifission channel requires a lot of time. Therefore one can suppose that in the DNS the thermal equilibrium could be realized, and the probability of formation of one or another configuration of the DNS is determined by the states density of the system. The statistical regularity of decay of the DNS formed in deep inelastic transfer reactions have been demonstrated by the Q_{gg} -systematics [22]. It is natural to assume that the probabilities for the DNS to go to the quasifission or the fusion channels are defined by the state densities of the system on the quasifission and fusion barriers, respectively.

Here some comments should be done. The term quasifission is used to describe the decay of the DNS into two nuclei-fragments comparable in mass, due to insufficient compactness of the system as compared with a fissile compound nucleus at the saddle point. In this case the DNS has such a form that it seems to be out of the fission barriers [23]. Such situation arises in collisions of massive heavy ions with heavy nucleus when the compound nucleus belongs to the region of transfermium elements. In the reactions $^{100}\text{Mo} + ^{100}\text{Mo}$ and $^{110}\text{Pd} + ^{110}\text{Pd}$ the compound nuclei ^{200}Po and ^{220}U

are strongly deformed at the saddle point, but the initial DNS has a more compact form. Consequently, at quasifission the system has to get over the potential barrier which depends on the spin of the system. In our calculations we assumed that the quasifission barriers for the system of $^{100}\text{Mo}+^{100}\text{Mo}$ and $^{110}\text{Pd}+^{110}\text{Pd}$ coincide with the fission barriers of the corresponding compound nuclei. The angular momentum influence on the height of the fission barrier has been taken into account following [24]. The top of the fusion barrier is slightly moving towards the greater asymmetry of the DNS with increasing l . To simplify our calculation, we fix the place of the potential barrier in the configuration with ^{48}Ca as a light nucleus.

Experimental measurements of the prefission neutron multiplicity ν_{pre} [21] demonstrated that even at hundreds of MeV of the excitation energy both the fission and the quasifission proceed relatively slowly. A large part of the excitation energy of the fissioning nucleus is taken away by neutrons so that at the saddle point the excitation energy is about 30-40 MeV [21]. Dominance of the quasifission channel upon the complete fusion channel in the reactions $^{100}\text{Mo}+^{100}\text{Mo}$ and $^{110}\text{Pd}+^{110}\text{Pd}$ means that the life time of the DNS in these reactions is determined mainly by the quasifission time. In our calculations, the system excitation energy for both channels of the reactions was taken equal to 35 MeV for all the initial excitation energies exceeding this value. The calculations have been performed also at the system excitation energy 50 MeV. The results are close to the results for 35 MeV.

The state densities on the top of the barriers of the quasifission and of the fusion are marked, respectively, by ρ_{B_f} and $\rho_{B_{fus}}$. For the description of state densities of the system of two interacting nuclei we use the following expression [25]

$$\rho_i(E^*) = \left(\frac{g^2}{g_1 g_2} \right)^{1/2} \frac{g}{6^{3/4} (2gE^*)^{5/4}} \exp [2(aE^*)^{1/2}], \quad (30)$$

where i corresponds to B_f or B_{fus} , g_1 and g_2 are the densities of the single-particle states near the Fermi surface for two nuclei of the DNS, $2g$ is the density of the single-particle states for a compound system. The ratio $\rho_{B_f}/(\rho_{B_{fus}} + \rho_{B_f})$ determines the quasifission probability, the ratio $\rho_{B_{fus}}/(\rho_{B_{fus}} + \rho_{B_f})$ is the fusion probability. Therefore the CNF cross section in the framework of the DNS-approach is determined by the multiplication of σ_c by last ratio.

In Figs.7,8 the results of the CNF cross section in the reactions $^{100}\text{Mo}+^{100}\text{Mo}$ and $^{110}\text{Pd}+^{110}\text{Pd}$ calculated in the framework of the DNS-approach with taking into account the competition between the complete fusion and the quasifission are presented.

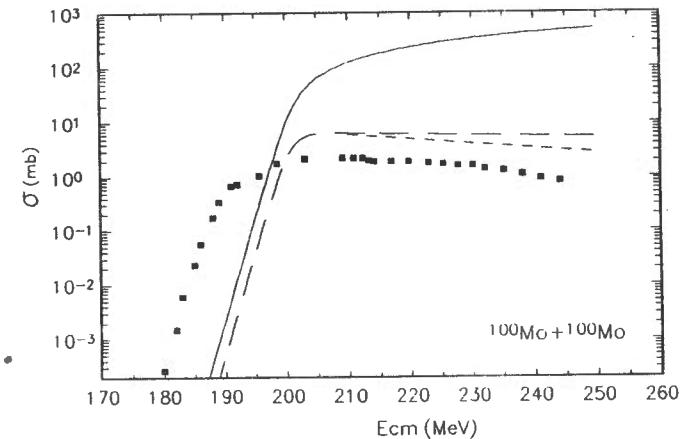


Fig.7. Calculated evaporation residue cross sections (short dashed line) and cross section of CNF (long dashed line) by using the DNS-approach for the reaction $^{100}\text{Mo}+^{100}\text{Mo}$. The experimental evaporation residue cross sections are presented by solid squares. The cross sections of CNF calculated in the framework of optic model are presented by solid line

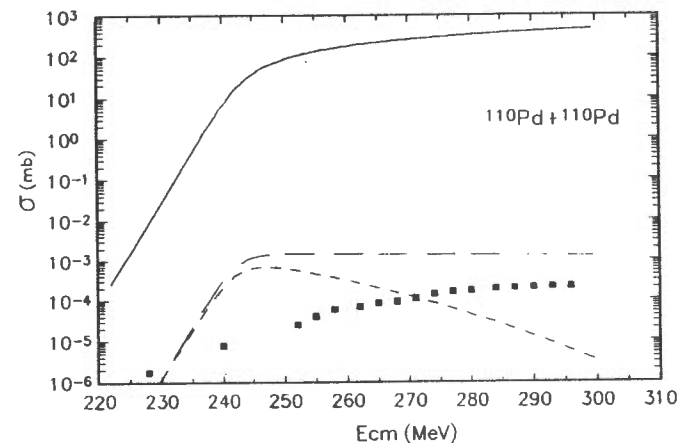


Fig.8. Same as Fig. 7, but for the reaction $^{110}\text{Pd}+^{110}\text{Pd}$

The data for σ_{cn} obtained in the framework of optical model are shown as well. The fusion barrier arising at the complete fusion of two massive nuclei abruptly diminishes the compound nucleus cross section. Unlike the macroscopic dynamic models [5-7], an increase in the kinetic energy of a collision does not change essentially the situation since the additional energy transforms into the DNS excitation and affects the competition of the complete fusion and the quasifission only through the DNS temperature.

3.3 Evaporation residue cross sections in the reactions $^{100}\text{Mo}+^{100}\text{Mo}$ and $^{110}\text{Pd}+^{110}\text{Pd}$

Once the data for the σ_{cn} are available, the evaporation residue cross sections in the reactions $^{100}\text{Mo}+^{100}\text{Mo}$ and $^{110}\text{Pd}+^{110}\text{Pd}$ can be calculated by using the scheme expounded in section 2.4. The results are presented in Figs.7,8. One can see that the DNS-approach allows one to obtain a much better agreement with the experiment than the traditional models of the complete fusion.

Calculations of the evaporation residue cross sections in the framework of the DNS-approach allow us to understand reasons of the sharp diminishing of cross sections in the transition from the reaction $^{100}\text{Mo}+^{100}\text{Mo}$ to $^{110}\text{Pd}+^{110}\text{Pd}$. In these reactions the mass and charge of compound nuclei are different only by 10% but the cross sections differ by several orders of magnitude. The dependence of the fusion barrier and the fission barrier on the angular momentum for both reactions is shown in Fig.9. One can see that the fission and fusion barriers change in the opposite directions: the fission barriers decrease in the transition from the reaction $^{100}\text{Mo}+^{100}\text{Mo}$ to the reaction $^{110}\text{Pd}+^{110}\text{Pd}$, and on the contrary the fusion barriers considerably increases.

In our calculations the proximity potential is used as $V_N(R)$. If we replace it by the folding-potential, the values of $\delta V(l)$ grow but the cross sections of the CNF decrease. So the total cross section of the massive nuclei fusion seems to be very sensitive to the potential $V_N(R)$. This fact can be used for the more precise definition of the potential $V_N(R)$.

The exchange with valence nucleons between the nuclei of the DNS increases the nuclear attraction [26]. One can expect that the number of the valence nucleons is larger for the symmetric configuration of the DNS than for the asymmetric one. The nucleon exchange between the DNS nuclei slightly increases the fusion barrier B_{fus} (due to lowering the bottom of the driving potential), however all the peculiarities of the fusion process seem to be conserved.

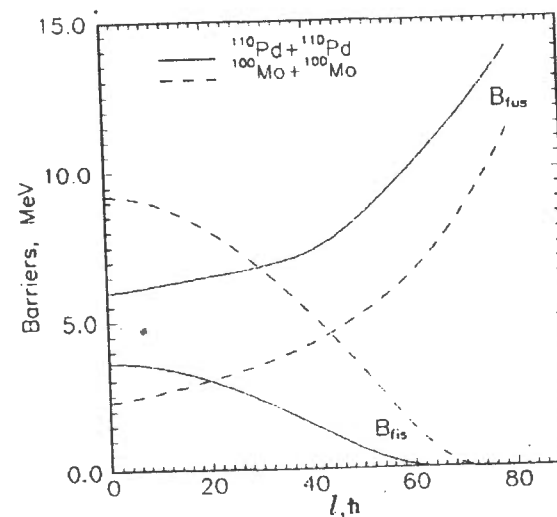


Fig.9. Dependence of fusion and fission barriers on angular momentum for the systems $^{100}\text{Mo}+^{100}\text{Mo}$ and $^{110}\text{Pd}+^{110}\text{Pd}$

The deformation of the DNS nuclei under the influence of the Coulomb forces slightly changes B_{fus} as well. This influence of the deformation has been estimated. It was supposed that in the symmetric DNS the nuclei look like rotating prolate ellipsoids with collinear located large axes. In both the reactions on the fusion barriers the light nucleus of the DNS was ^{48}Ca while the heavy nuclei were ^{152}Er and ^{172}Hf (if the particle evaporation is neglected). For this configuration the deformation is introduced only for heavy nuclei of the DNS. The surface of the deformed nucleus is described by the expression:

$$R_{id} = fR_i(1 + \beta Y_{20}(\theta, \varphi)), \quad (31)$$

$$f = \left[\left(1 + \beta \sqrt{\frac{5}{4\pi}}\right) \left(1 - \beta \sqrt{\frac{5}{16\pi}}\right)^2 \right]^{-1/3},$$

The factor f is introduced for the volume conservation. Calculations of B_{fus} were performed with $V_N(R)$ in the "proximity" form. In (25) \bar{R} has been modified according to [27]. The potential of the Coulomb interaction $V_C(R)$ was calculated following [27], as well. In $V(Z, l)$ the corresponding changes have been done in the components describing the surface and the Coulomb energies. For the symmetric configuration of the DNS the value $\beta = 0.2$ was taken; and for the BG point, $\beta = 0.4$, which is

in accordance with the data on the deformation in symmetric and asymmetric fission [28]. By our estimations the deformation of the DNS nuclei increases B_{fus} nearly by 2 MeV for the reaction $^{110}\text{Pd}+^{110}\text{Pd}$ and by 1 MeV for $^{100}\text{Mo}+^{100}\text{Mo}$.

4. Conclusion

In the paper the experimentally measured cross sections of the evaporation residue in the reactions $^{100}\text{Mo}+^{100}\text{Mo}$ and $^{110}\text{Pd}+^{110}\text{Pd}$ are compared with the results calculated in the framework of different models of complete fusion. This comparison allows us to estimate the validity of the CNF mechanism suggested in several models.

The determination of the evaporation residue cross sections includes the calculation of the CNF cross section and the competition between fission and emission of light particles, γ -rays at the compound nucleus de-excitation. The CNF cross sections have been calculated in the framework of several models of complete fusion and the de-excitation of a compound nucleus has been calculated on the basis of the Monte-Carlo method.

The calculated results are obtained by using the optical model; the model with surface friction and the macroscopic dynamic model seem to be in sharp contradiction with the experimental data. Especially for the reaction $^{110}\text{Pd}+^{110}\text{Pd}$ the calculated evaporation residue cross sections exceed the experimental value by several orders of magnitude.

The analysis of the complete fusion in the systems $^{100}\text{Mo}+^{100}\text{Mo}$ and $^{110}\text{Pd}+^{110}\text{Pd}$ on the basis of the DNS-approach revealed an important specific feature of this process, the appearance of the fusion barrier on the way of the DNS evolution to a compound nucleus. As a result, the competition between the channels of quasifission and complete fusion arises and reduces strongly the CNF cross section. This is a basic result which qualitatively distinguishes the DNS-approach from other models of fusion. The calculations of the evaporation residues cross section in the reactions $^{100}\text{Mo}+^{100}\text{Mo}$ and $^{110}\text{Pd}+^{110}\text{Pd}$ on the basis of the DNS-approach lead to satisfactory agreement with the experimental data, which can be considered as an evidence of the validity of our concept of the CNF mechanism developed in the DNS-approach.

References

1. Galin, J., Gurreau, D., Lefort, U., Tarrago, X.: Phys. Rev. C9, 1081 (1974)
2. Iljinov, A.S., Chereponov, E.A.: JINR Communication P7-84-68, Dubna, 1984
3. Gross, D.H.E., Nayak, R.C., Satpathy, L.: Z. Phys. A—Atomic and Nuclei 299, 63 (1981)
4. Fröbrich, P.: Phys. Rep. 116, 337 (1984)
5. Swiatecki, W.J.: Phys. Scripta 24, 113 (1981)
6. Bjornholm, S., Swiatecki, W.J.: Nucl. Phys. A391, 471 (1982)
7. Blocki, J.P., Feldmeier, H., Swiatecki, W.J.: Nucl. Phys. A459, 145 (1986)
8. Volkov, V.V.: Nucleus-Nucleus Collision II. Visby, 1985, v.1, Contributed Papers, North-Holland, 1985, p.54; Volkov, V.V.: Izv. AN SSSR ser. fiz. 50, 1879 (1986); Volkov, V.V.: Intern. School-Seminar on Heavy Ion Physics, Dubna, September 23–29, 1986, D7-87-68, Dubna 1987, p.528; Volkov, V.V.: Proc. of the 6th Intern. Conf. on Nuclear Reaction Mechanisms. Ed. by E.Gadioli, Varenna, June 10–15, 1991. Ricerca Scientifica ed Educazione Permanente Supplemento n. 84, 1991, p.39
9. Morawek, W., Ackermann, T., Brohn, T., Clerc, H.G., Gollerthan, U., Hanlet, E., Horz, M., Schwab, W., Voss, B., Schmidt, K.H., Gaimard, J.J., Hesberger, F.P.: GSI Scientific Report 1988, p.38; Schmidt, K.H., Morawek, W.: Rep. Prog. Phys. 54, 949 (1991)
10. Iljinov, A.S., Chereponov, E.A.: INR Preprint P-0090, Moscow, 1978
11. Iljinov, A.S., Oganesyan, Yu. Ts., Chereponov, E.A.: Sov. J. Jad. Fiz. 36, 118 (1982)
12. Bass, R.: Nuclear Reactions with Heavy Ions, Berlin, Heidelberg, New York: Springer 1980
13. Dostrovsky, I.: Phys. Rev., 111, 1659 (1958)
14. Blann, M., Plasil, F.: Phys. Rev. Lett., 29, 303 (1972)
15. Ignatyuk, A.V.: Statistical properties of excited nuclei. Moskow: Energoizdat 1983 (in russian)

16. Myers, W.D.: Droplet model of atomic nucleus. New York: IFI/Plenum Press 1977
17. Schmidt, R., Teichert, J.: JINR Communication E4-80-527, Dubna
18. Migdal, A.B.: Theory of finite Fermi systems and applications to atomic nuclei. Moscow: Nauka 1988 (in russian)
19. Antonenko, N.V., Jolos, R.V.: Z. Phys. A—Hadrons and Nuclei **339**, 453 (1991)
20. Bondorf, J.P., Sobel, M.I., Sperber, D.: Phys. Rep. **15**, 83 (1974)
21. Hinde, D.J., Hilsher, D., Rossner, H.: Nucl. Phys. A **502**, 497c (1989)
22. Volkov, V.V.: Phys. Rep. **44**, 93 (1978)
23. Ngo, Ch.: Progr. Part. Nucl. Phys. **16**, 139 (1986)
24. Sierk, A.J.: Phys. Rev. C **33**, 2039 (1986)
25. Ayik, S., Schürman, B., Nörenberg, W.: Z. Phys. A—Atomic Nuclei **277**, 299 (1976)
26. Jolos, R.V., Nasirov, A.K.: Sov. J. Jad. Phys. **45**, 1298 (1987)
27. Malhotra, N., Gupta, R.K.: Phys. Rev. C **31**, 1179 (1985)
28. Hasse, R.V.: Sov. J. Question of Atomic Science and Technology ser. Nuclear Constant, **1**, 3 (1988)

Received by Publishing Department
on May 19, 1992.

WILL YOU FILL BLANK SPACES IN YOUR LIBRARY?

You can receive by post the books listed below. Prices — in US \$, including the packing and registered postage.

D13-85-793	Proceedings of the XII International Symposium on Nuclear Electronics, Dubna, 1985.	14.00
D1,2-86-668	Proceedings of the VIII International Seminar on High Energy Physics Problems, Dubna, 1986 (2 volumes)	23.00
D3,4,17-86-747	Proceedings of the V International School on Neutron Physics. Alushta, 1986.	25.00
D9-87-105	Proceedings of the X All-Union Conference on Charged Particle Accelerators. Dubna, 1986 (2 volumes)	25.00
D7-87-68	Proceedings of the International School-Seminar on Heavy Ion Physics. Dubna, 1986.	25.00
D2-87-123	Proceedings of the Conference "Renormalization Group-86". Dubna, 1986.	12.00
D2-87-798	Proceedings of the VIII International Conference on the Problems of Quantum Field Theory. Alushta, 1987.	10.00
D14-87-799	Proceedings of the International Symposium on Muon and Pion Interactions with Matter. Dubna, 1987.	13.00
D17-88-95	Proceedings of the IV International Symposium on Selected Topics in Statistical Mechanics. Dubna, 1987.	14.00
E1,2-88-426	Proceedings of the 1987 JINR-CERN School of Physics. Varna, Bulgaria, 1987.	14.00
D14-88-833	Proceedings of the International Workshop on Modern Trends in Activation Analysis in JINR. Dubna, 1988	8.00
D13-88-938	Proceedings of the XIII International Symposium on Nuclear Electronics. Varna, 1988	13.00
D17-88-681	Proceedings of the International Meeting "Mechanisms of High-T _c Superconductivity". Dubna, 1988.	10.00
D9-89-52	Proceedings of the XI All-Union Conference on Charged Particle Accelerators. Dubna, 1988 (2 volumes)	30.00
E2-89-525	Proceedings of the Seminar "Physics of e ⁺ e ⁻ Interactions". Dubna, 1988.	10.00
D9-89-801	Proceedings of the International School-Seminar on Heavy Ion Physics. Dubna, 1989.	19.00
D19-90-457	Proceedings of the Workshop on DNA Repair on Mutagenesis Induced by Radiation. Dubna, 1990.	15.00